

# SYNTHESIS OF SILICA NANOPARTICLES VIA GREEN APPROACH BY USING HOT AQUEOUS EXTRACT OF *THUJA ORIENTALIS* LEAF AND THEIR EFFECT ON BIOFILM FORMATION

M.Th.AL-Azawi<sup>1</sup> S.M.Hadi<sup>2</sup> Ch.H.Mohammed<sup>3</sup>

Researcher Asst. Prof Asst. Prof

Dept. of Physics<sup>1,3</sup> and Biology<sup>2</sup>- Coll. of Science - Univ. of Baghdad

[mthamir50@gmail.com](mailto:mthamir50@gmail.com), [sabahtech2013@gmail.com](mailto:sabahtech2013@gmail.com), [ghuson.hamed@yahoo.com](mailto:ghuson.hamed@yahoo.com)

## ABSTRACT:

There is great interest for NPs manufacturing by environmentally friendly and economic manner. The aqueous leaves extract of *Thuja orientalis* was used to synthesized silica nanoparticles (SiO<sub>2</sub>NPs) by using two green methods, the first one is the magnetic stirrer method and the second method by using the cold plasma. The XRD pattern for both samples annealed at T<sub>a</sub>=600°C for 1h, while they showed the characteristic of Bragg peaks for poly phases at (001), (010), (10-1), (1-10), (0-12) and (002) for SiO<sub>2</sub> triclinic (anorthic). The average crystalline size was calculated by using Scherer's formula, which was 11.1868 nm in magnetic stirrer method, while the cold plasma method showed amorphous structure. The morphology analysis using atomic force microscopy showed that the grain size was 33.94 and 18.37 nm for magnetic stirrer and cold plasma methods respectively. Fourier Transform Infrared Spectroscopy (FTIR) analysis indicates hydrophilic functional groups in the capping matrix, which can improve the stability of silica NPs. The biofilm inhibition of silica NPs were investigated for two genus of bacteria *Staphylococcus aureus* and *Escherichia coli*, the green silica NPs that synthesized by using cold plasma method showed the highest inhibition effect on *S. aureus* and *E. coli* respectively.

**Keywords:** green synthesis, annealed, cold plasma, magnetic stirrer, bacteria.

العزوي وآخرون مجلة العلوم الزراعية العراقية- 2019: 50(عدد خاص):245-255

تحضير دقائق السليكا النانوية بالطريقة الخضراء باستعمال المستخلص المائي الساخن لأوراق التويا الشرقية وتأثيرها على تشكيل الغشاء الحيوي.

مريم ثامر العزوي صباح مهدي هادي غصون حميد محمد

باحث استاذ مساعد استاذ مساعد

قسم الفيزياء<sup>١</sup> وعلوم الحياة<sup>٢</sup>-كلية العلوم- جامعة بغداد

المستخلص

هناك اهتمام بتحضير الدقائق النانوية بطريقة اقتصادية وصديقة للبيئة. حضرت دقائق السليكا النانوية (SiO<sub>2</sub>NPs) باستعمال مستخلص أوراق التويا الشرقية وباستعمال طريقتين خضراء، الطريقة الاولى هي طريقة المحرك الممغنطيسي والثانية هي طريقة البلازما الباردة. فحص تركيب الدقائق باستعمال تقنية حيود الاشعة السينية (XRD) لكلا النموذجين المدن عند درجة حرارة 600 درجة مئوية ولمدة ساعة واحدة، اظهرت قمم براك المميزة امتلاكها طور متعدد البلورات (001)، (010)، (10-1)، (1-10)، (0-12)، (002) للسليكا ثلاثية الميل (anorthic). حسب متوسط حجم البلورة باستخدام معادلة شرر وكان حجمها 11.1868 nm بطريقة المحرك المغناطيسي، بينما اظهرت طريقة البلازما الباردة تركيب عشوائي للبلورة. اظهر تحليل المورفولوجيا باستعمال مجهر القوة الذرية ان الحجم الحيوي هو 33.94، 18.37 nm بطريقتي المحرك المغناطيسي والبلازما الباردة بالتتابع. يشير التحليل الطيفي للأشعة تحت الحمراء (FTIR) الى وجود مجموعات وظيفية محبة للماء في مصفوفة القنص التي يمكن ان تحسن استقراره دقائق السليكا النانوية. فحص تثبيط تكوين الغشاء الحيوي بتأثير دقائق السليكا النانوية تجاه جنس من البكتريا هما المكورات العنقودية الذهبية والاشريكية القولونية. اظهرت دقائق السليكا النانوية الخضراء المحضرة باستعمال طريقة البلازما الباردة تأثير تثبيطي اعلى على البكتيريا الموجبة والسالبة لملون جرام (المكورات العنقودية الذهبية والاشريكية القولونية) بالتتابع.

كلمات مفتاحية: التحضير الاخضر، التلدين، البلازما الباردة، المحرك المغناطيسي، جراثيم.

\*Received:5/5/2018, Accepted:19/9/2018

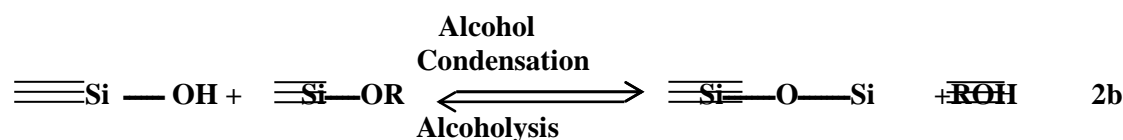
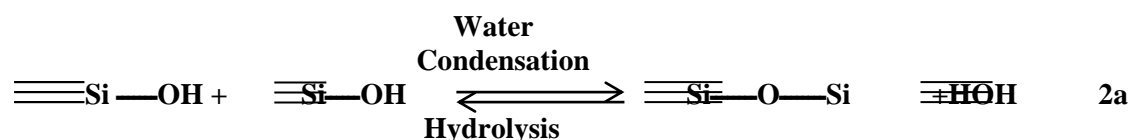
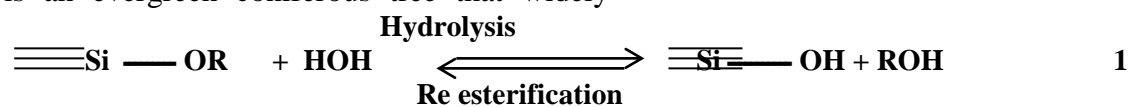
## INTRODUCTION

Nanotechnology is the most growing, widespread scientific and technical achievement in the world. This science was emerged by applying of nanosize structures as a solution to the previous difficult problems. Different fluorescent silica NPs with similar composition and functionalization have emerged as a particularly fascinating fluorescent probe and attracted widespread interest in biology and medicine (41,50). Silica NPs have high thermal, chemical stability, high surface area and good biocompatibility, but nude silica NPs shows no detrimental effects on bacteria. Sometimes silica NPs may be used as a mediator to enhance delivery doses of antimicrobials such as copper, zinc and silver NPs at the target sites and therefor reduce the antibiotics doses intake (20). Most of the chemical methods that used for the synthesis of NPs are too expensive and also involve the use of toxic, hazardous chemicals that are responsible for various biological risks. This enhances the growing need to develop environmentally friendly processes through green synthesis and other biological approaches. Sometimes the synthesis of NPs using various plants extract can be more useful than the other biological methods, which involve very complex procedures of maintaining microbial cultures. On the other hand the using of plant extracts is the most adopted method because the plants are widely distributed, available and much safer to handle. In addition, the plants have various secondary metabolites compounds that consider as another source for natural reducing and capping agents (22). *Thuja orientalis* plant is an evergreen coniferous tree that widely

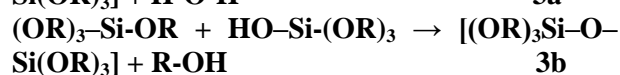
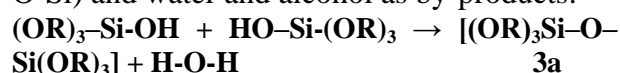
distributed in East Asia (53), it belongs to Cupressaceae family and used in landscape. *T. orientalis* leaves have essential oils which are used in traditional medicine as antifungal, bactericide and other properties like eradicate parasitic worms. Normally the oil is toxic, mainly for the presence of  $\alpha$ - thujone, the other leaves compounds are; rhodoxanthin, amentoflavone, hinokiflavone, quercetin, myricetin, carotene, xanthophylls and ascorbic acid (10,49). In this study, we have used the green method in synthesis of silica NPs using *T. orientalis* aqueous leaf extract and TEOS for silica precursor as a sustainable, cheap and available material for synthesis of silica NPs in an environmentally friendly manner.

### Synthesis chemistry of silica

The magnetic stirrer and cold plasma methods means the synthesis of an inorganic network by a chemical reaction produced in the solution at low temperature. The major advantage of this method is that it offers the possibility to obtain hyaloids solids, which are very difficult to be obtained by conventional techniques of burning at high temperatures and offers the possibility to obtain materials with predetermined structure, depending on the conditions of the experiment. The development of silica synthesis process in materials science starts with a solution of silicon alkoxide compound  $\text{Si}(\text{OR})_n$  as a precursor that melted in an alcohol or other low-molecular weight organic solvent, were R is an alkyl group ( $\text{C}_x\text{H}_{2x+1}$ ) (8,52). Compared with colloid chemistry, the alkoxide route can be more easily controlled by controlling hydrolysis 1 and condensation reactions (2a-water condensation, 2b-alcohol condensation)



The hydrolysis reaction 1-4, consists in replacing of the alkoxide groups (-OR) with hydroxyl groups (-OH) and releasing of the corresponding ROH alcohol molecules. A complete hydrolysis 4 is obtained when the stoichiometric molar ratio water: Si(OR)<sub>n</sub> is 4. Any intermediate species [(OR)<sub>2</sub>-Si-(OH)<sub>2</sub>] or [(OR)<sub>3</sub>-Si-(OH)] would be considered the result of partial hydrolysis 3a, 3b. A small amount of water leads to a slow hydrolysis due to the reduced reactant concentration. A large amount of water gives a slow hydrolysis due to the increased reactant dilution. Subsequent condensation reactions involve the silanol groups (Si-OH), produce siloxane bonds (Si-O-Si) and water and alcohol as by-products:



#### Floating electrode dielectric barrier discharge (FE-DBD) plasma technique

The samples were prepared by using the floating electrode dielectric barrier discharge (FE-DBD) plasma technique, which was manufactured by Dr. Hamid H. Murbit in the College of Science for Women/University of Baghdad. The floating electrode dielectric barrier discharge (FE-DBD) system, constructed similarly to conventional dielectric barrier discharges (DBDs) is inherently offers better potential for diversity, since it works in room temperature, air (normal atmospheric pressure) and it has a cold touch (15,29). This system operates at power densities of 0.1-2 W/cm<sup>2</sup>. FE-DBD operates under the conditions where one of the electrodes is a dielectric-protected powered electrode and the second active electrode is the organ, liquid surface, animal or human skin without second surface present discharge does not ignite (22). In the FE-DBD setup, the second electrode is not grounded and remains at a floating potential. Of note is the fact that FE-DBD is completely safe from the electrical perspective and non-damaging for application to animal or human skin delicate surfaces which are likely to be damaged by thermal (hot) plasma. Discharge ignites when the powered electrode approaches the surface to be estimated (treated) at a distance (discharge gap) less than

about 3 mm, depending on the form, duration, and polarity of the driving voltage (26). Power deposited into plasma discharge gap was analyzed by measuring current passing through the discharge gap and the voltage drop in the gap (17).

#### MATERIALS AND METHODS

Tetraethyl orthosilicate (TEOS) was obtained from (Aldrich chemical, purity > 98%). All the glass-wares were washed with concentrated hydrochloric acid then deionized water (diH<sub>2</sub>O). The Milli-Q ultrapure deionized water with electrical conductivity (E.c = 0.7 μs cm<sup>-1</sup>) was used for the all purposes.

#### Preparation of *T. orientalis* aqueous leaf extract

The leaves of *T. orientalis* were collected from the University of Baghdad gardens. Plant parts were washed several times by using tap water then by distilled water to remove all dirt then dried at room temperature. The samples were grinded into powder by using electrical grinder; 10 gm of dried powder was added to 100 ml of diH<sub>2</sub>O. After boiling for 10 min then homogenized on the magnetic stirrer for 4h then the mixture was filtered with filter paper Whatman No.1. The extract was centrifuged at 5000 rpm for 15 min and stored at 4 °C until use.

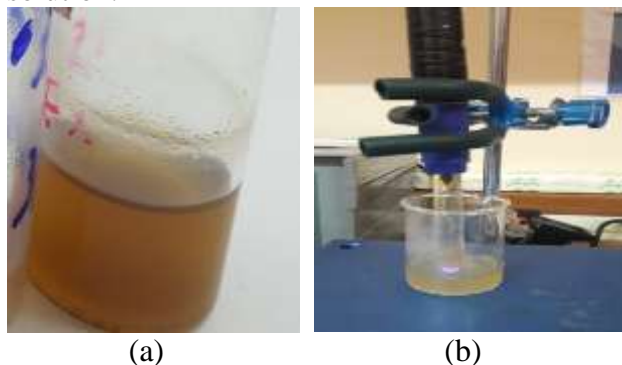
#### Preparation of green silica nanoparticles by using magnetic stirrer method

Silica NPs were synthesized by added 15 ml of TEOS (10<sup>-3</sup>M) as silica precursor in a flask placed in a water bath with continuous stirring until the temperature stabilized at 60°C then 5 ml of *T. orientalis* aqueous leaf extract was added. The reaction was lasted for 30 min with continuous stirring, as shown in Figure 1a.

#### Preparation of green silica nanoparticles by using cold plasma method

Silica NPs were synthesized by added 15 ml of TEOS (10<sup>-3</sup>M) with 5ml of *T. orientalis* leaf extract, the mixture was left under the influence of plasma electrode for 5 min. In this experiment, continuous wave plasma high voltage (4 kV) was applied to a quartz protected electrode that generates plasma between the quartz and the liquid surface as shown in figure (1b). Discharge ignites when the powered electrode approaches the surface to be estimated (treated) at a distance (discharge gap) less than about 2 mm. In this

way, we obtain a light yellow nanoparticle solution.



(a) (b)  
**Figure 1. Green synthesis of SiO<sub>2</sub> NPs. a) Synthesis SiO<sub>2</sub> NPs by using magnetic stirrer method. b) Synthesis SiO<sub>2</sub> NPs by using cold plasma method**

#### **Determination of antimicrobial activity by agar well diffusion method**

The antimicrobial activity of silica nanoparticles were determined by using agar diffusion method against the pathogenic bacteria isolates (*S. aureus* and *E. coli*). The Muller Hinton Agar plates were inoculated with  $0.5 \times 10^8$  (CFU/ml) of *S. aureus* and *E. coli* strain by using cotton swabs under aseptic conditions.

#### **The effect of silica nanoparticles on biofilm formation**

Biofilm formation assays were performed using 96- well microtiter plate, based on the protocol by Goh, S. et al (19), with slight modifications. *E. coli* and *S. aureus* bacteria were cultured in tryptone soya broth (TSB) for 18-24 hrs and the resulting culture was adjusted to 0.5 McFarland tube. All the wells of microtiter plate were loaded with 100µl of TS broth with 100 µl of nanoparticles solution except the control filled only TS broth, then the plate was incubated at 37°C for 24 h. All the NPs samples were tested three times. The microbial planktonic was removed by upset the plate over a waste tray then 0.1% w/v crystal violet solution was added to each well and left for 10 min at room temperature. The dye was removed by submerging the plate in a water tray, then was inverted and left in air to dry. The wells were treated with 95% v/v ethanol for 10 min to solubilize the dye. Optical density (OD) was measured at 630 nm (1).

## **RESULTS AND DISCUSSION**

### **X-ray diffraction analysis**

The diffraction pattern gives information on translational symmetry - size and shape of the unit cell from peak positions and information on electron density within the unit cell, namely, where the atoms are located from peak intensities. It also, gives information on the deviations of perfect particles, if the size is less than approximately 100-200 nm, extended defects and micro strain from peak shapes and widths (28). Figure 2 shows the XRD pattern for samples which are prepared by tow method magnetic stirrer and cold plasma using the *T. orientalis* leaves extract in green method, annealed to 600°C for 1h (5). All parameters value resulted from XRD is shown in Table 1. It can be observed that all diffraction peaks of poly phases (001), (010), (10-1), (1-10), (0-12) and (002) facets can be indexed as the typical triclinic structure for silica. The crystallite sizes of silica NPs calculated for all peaks by using Scherer's formula. It was found that the value of average crystalline size 11.1868 nm because this the size that lies within the NPs as shown in Table 1, these results are agreed with Boisen M. B. et al. (6). While The XRD diffractogram for synthesis silica NPs by using cold plasma is shown in Figure 2. which released that the broad peak in the diffraction angle range of ( $2\theta=15-30^\circ$ ) who is centered at  $23^\circ$  attributed to the amorphous structure for SiO<sub>2</sub> NPs, without any defined peaks due to the existing of crystalline structure (18,32). The production of amorphous silica nanoparticles contributed to the positive impact as it has broad applications in our daily life. This is due to the special characteristics of amorphous silica nanoparticles that are stable in a long time compared to the crystalline silica (3). Secondly, amorphous silica is more reactive than crystalline silica. This is because of the hydroxyl group in the amorphous region is more applicable to use in the reaction compared to their crystalline region (51). These results were agreed with Mohd N. K. et al. (36).

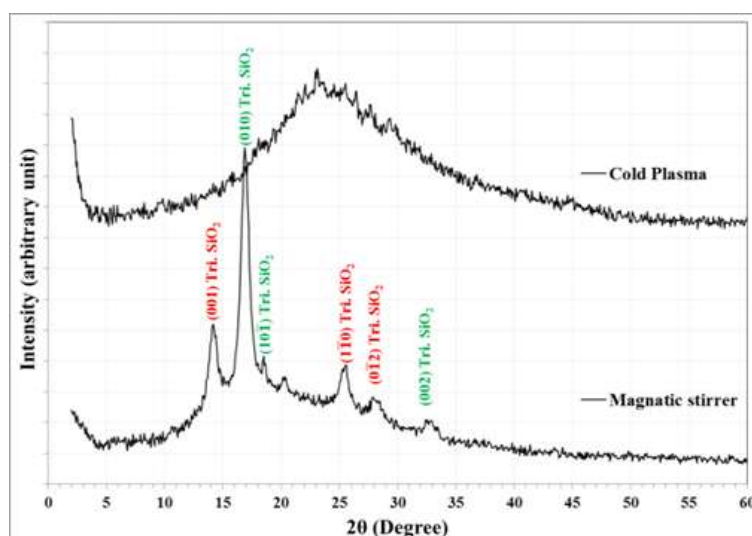


Figure 2. The XRD pattern of SiO<sub>2</sub> NPs green synthesis

Table 1. X-ray diffraction data for Silica NPs

Synthesis methods	2θ (Deg.)	FWHM (Deg.)	d <sub>hkl</sub> Exp.(Å)	G.S (nm)	hkl	d <sub>hkl</sub> Std.(Å)	Phase	Card No.
Magnetic stirrer	14.1683	0.7593	6.2460	10.5	(001)	6.2332	Tri. SiO <sub>2</sub>	96-900-6299
	16.9059	0.7781	5.2402	10.3	(010)	5.2328	Tri. SiO <sub>2</sub>	96-900-6301
	18.5419	0.3981	4.7814	20.2	(10-1)	4.8181	Tri. SiO <sub>2</sub>	96-900-6301
	25.4311	0.9279	3.4996	8.8	(1-10)	3.4707	Tri. SiO <sub>2</sub>	96-900-6299
	28.1547	1.3549	3.1669	6.0	(0-12)	3.1729	Tri. SiO <sub>2</sub>	96-900-6299
	32.5	1.3010	2.7570	6.4	(002)	2.7228	Tri. SiO <sub>3</sub>	96-900-6301
Cold plasma					Amorphous			

#### Atomic force microscopy (AFM) measurement

Two and three dimensional (2D and 3D) profile of AFM was used to give information of surface morphology to materials. Figure 3a shows the surface morphology of silica NPs prepared by hydrothermal method, which notes that the particles were spherical, while Figure 3b refers to the granular distribution of silica NPs. Figure 4a show 2D and 3D the atomic force microscopy images that synthesized by using cold plasma method, it was observed that the shape of the particles was spherical. While Figures 4b refer to the granular distribution of silica nanoparticles of the same method. It is found the size of the grains was 33.94 nm and 18.37 nm for the samples that prepared by using the magnetic stirrer and cold plasma method respectively. The smaller silica nanoparticles have many positive attributes, such as good chemical stability and biofilm, which would make them suitable for many practical applications.

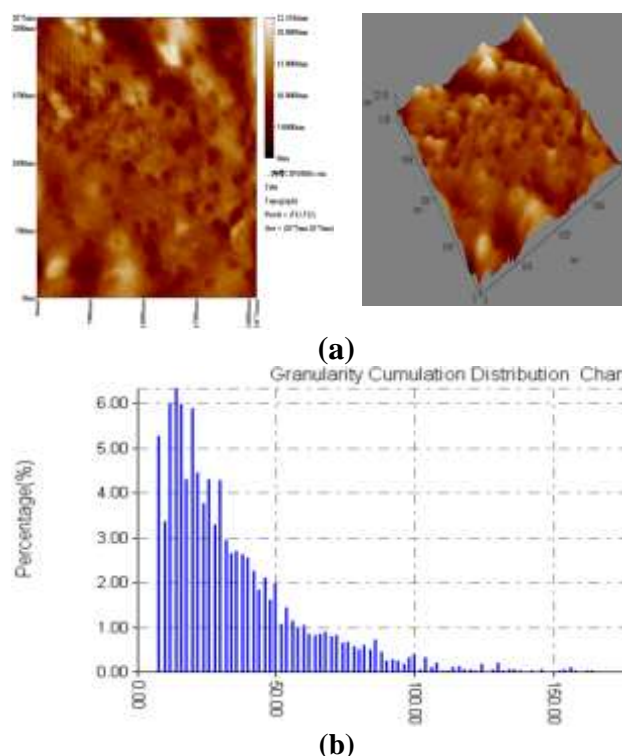
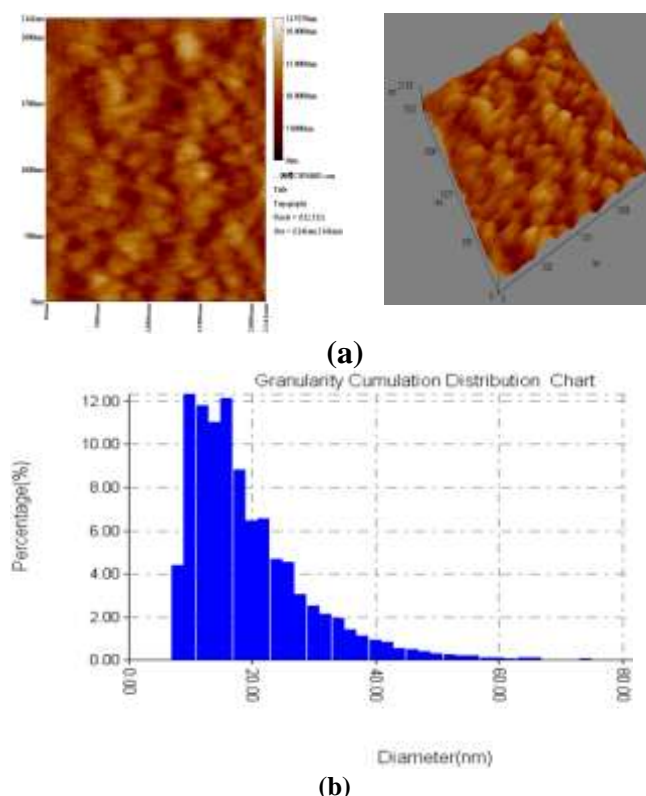


Figure 3. (a) 3D& 2D AFM images of SiO<sub>2</sub> NPs by using magnetic stirrer method. (b) Granularity distribution of SiO<sub>2</sub> NPs by using magnetic stirrer method.



**Figure 4. (a) 3D& 2D AFM images of SiO<sub>2</sub> NPs by using cold plasma method. (b) Granularity distribution of SiO<sub>2</sub> NPs by using cold plasma method.**

AFM imaging of the nanoparticles was performed by drying on a clean glass slide substrates. The surface morphology has been investigated using images of AFM which produces topological images of surface at very high magnification. Images of AFM are widely known, providing a useful tool for unambiguously describing the size and distribution of nanoparticle size. The results of AFM measurement are shown in Table 2. The increase in grain size of SiO<sub>2</sub> NPs by using magnetic stirrer method by is due to the increasing temperature of the magnetic stirrer (37).

**Table 2. The grain size of SiO<sub>2</sub> NPs**

Synthesis methods	Average grain size (nm)
Magnetic stirrer	33.94
Cold plasma	18.37

From the above table it can be noted the increasing that happened in grain size for the samples was prepared by green method that used the magnetic stirrer due to the use of temperature in preparation, where high temperature increases crystalline growth of the material, so there is an increase in grain size.

**Fourier transform infrared spectroscopy (FTIR)**

The compounds were characterized via FTIR in Shimadzu IR-Affinity-1 (Japan) Spectrometer. The samples were mixed with potassium bromide and examined directly in their powder state without further preparation. The FTIR measurements of biosynthesized silica NPs were carried out to identify the possible interaction between protein and silica NPs. Results of FTIR study showed sharp absorption peaks located at about (1626, 1606.7 and 1608.6) and (3423.65, 3404.36 and 3398.57) cm<sup>-1</sup> Figures 5. Absorption peak at (1626, 1606.7 and 1608.6) cm<sup>-1</sup> may be assigned to the amide I bond of proteins arising due to carbonyl stretch in proteins, and peaks at (3423.65, 3404.36 and 3398.57) cm<sup>-1</sup> are assigned to OH stretching in alcohols and phenolic compounds (25). The absorption peak at (1626, 1606.7 and 1608.6) cm<sup>-1</sup> is close to that reported for native proteins (33). This evidence suggests that proteins are interacting with biosynthesized nanoparticles and also their secondary structure was not affected after binding with NPs (14). Phenolic compounds belonging to the lignin's group have been earlier reported to be capable of chelating with elements to form complexes (7). Thus, it can be concluded that hydroxyl and carboxyl groups present in phenolic compounds of the *T. orientalis* leaf extract. These results confirm the presence of phenols and proteins which may act as stabilizing agents for NPs (47). Broad peak was observed around 3466 cm<sup>-1</sup> proved the presence of O-H stretching vibration due to the vibration of the silanol group on the silica surfaces. This finding was consistent with the previous study reported on silica NPs (2). Both of the spectra of silica NPs synthesis do not show any significant difference to each other.

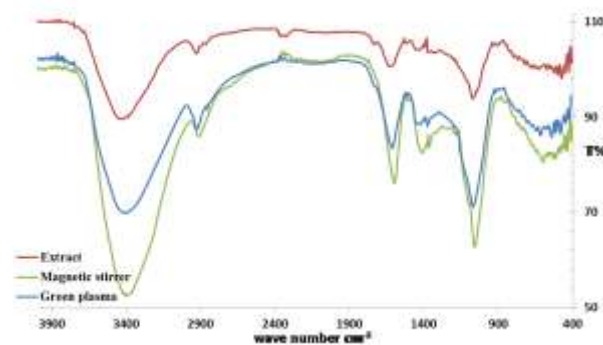


**Figure 5. FTIR spectra for prepared SiO<sub>2</sub> NPs**

Table 3. FTIR data for SiO<sub>2</sub> NPs

Bonds	Aqueous leaf extract	Magnetic Stirrer	Cold plasma
	wave number cm <sup>-1</sup>		
Si-O-Si bending (35,42,24)		451.34	478.35
Si-H bond (21,31)		617.22	615.29
Shoulder (Si-O-Si) asymmetric stretch (36,42,21,31,40,39,4,46,27)	1066.64	1070.49	1064.71
C-N stretch (aromatic amines) (47)	1384.50	1377.17	1375.25
C-H bending (46,11)	1436.97		
The amide I bond of proteins arising due to carbonyl stretch in proteins (11,12,13,28,47)	1625.99	1606.70	1608.63
-COO- groups (35)	1732.08		
CO vibration (30,38)	2364.73		
C=O vibrations (35)	2927.94	2931.80	2918.30
Silanol (Si-O) stretch and Absorb H <sub>2</sub> O on surface or -OH stretching and phenolic compounds with strong H bond (36,47,2,25) O-H stretching vibration due to the vibration of the silanol group on the silica surfaces.	3423.65	3404.36	3398.57

### The effect of SiO<sub>2</sub> NPs on biofilm formation

The results showed that a difference found in biofilm formation depends on the grain size of nanoparticles and the genus of bacteria as shown in Table 4. Each of the samples of silica nanoparticles that synthesized by using magnetic stirrer and cold plasma methods with *Thuja orientalis* aqueous leaf extract presented high inhibition effect against the entire bacteria compared with the control. The silica nanoparticles that synthesized by using cold plasma method had displayed the highest inhibition effect on the formation of biofilm by *S. aureus* and *E. coli* compared with the control (0.1035, 0.07, 0.2773 and 0.2), and then followed by aqueous leaf extract of *Thuja orientalis* that presented inhibition effect against the biofilm formation (0.12, 0.125, 0.2773 and 0.2) respectively on the bacteria.

Table 4. The effect of different SiO<sub>2</sub> NPs on biofilm growth on bacteria

Bacterial species	<i>S. aureus</i>	<i>E. coli</i>
	O.D 630nm	
Control	**0.2773	*0.2
Aqueous leaf extract	0.12	0.125
Magnetic stirrer	0.146333	0.143333
Cold plasma	0.1035	0.07

Standard deviation (S.D): 0.153

Cut-Off: 0.567

\* moderate biofilm producer

\*\* strong biofilm producer

Accordingly, isolates were classified as follows: O.D < 0.12 = no biofilm producer or weak biofilm producer, 0.12 < O.D ≤ 0.24 = moderate biofilm producer and 0.24 < O.D = strong biofilm producer (34). All the samples of SiO<sub>2</sub> NPs showed high effect against *S.*

While the silica NPs that synthesized by using magnetic stirrer method had less effect on biofilm formation compared with the control (0.146333, 0.143333, 0.2773 and 0.2) respectively as shown in Figure 6.

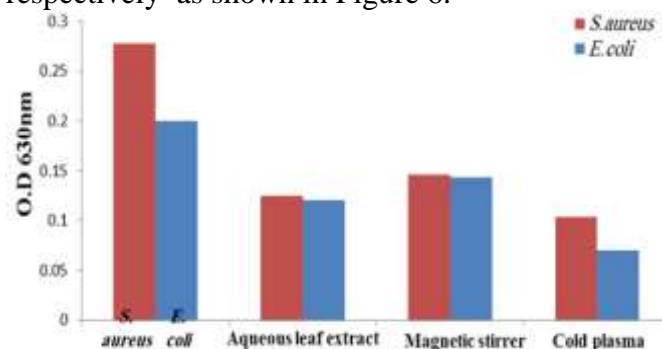


Figure 6. The differences in biofilm formation for bacteria after treatment with different SiO<sub>2</sub> NPs

*aureus* biofilm formation compared with the control as shown in Table 4, while silica NPs that synthesized by using cold plasma method offered highest inhibition effect for biofilm growth than the rest of the samples because of the less average grain size of silica and then the extract of *Thuja orientalis* as shown in Figure 6. Based on the differences in the structure of the bacteria cell wall, they are

classified as gram negative or positive. The structural differences lie in the organization of a key component of the membrane, peptidoglycan. These differences in the cell wall confer different properties to the cell, in particular responses to external stresses, including heat, UV radiation and antibiotics (44). The differences in biofilm formation between the gram negative bacteria and positive bacteria may due to the differences in cell wall composition, the structure of the cell wall play an important role in tolerance or susceptibility of bacteria in the presence of nanoparticles and its diffusion inside biofilm matrixes by altering surface from hydrophilic to a highly hydrophobic towards nanoparticles due to change expression of cell wall proteinase. Silica NPs have high surface area, and good biocompatibility, so they found that silica NPs inhibit bacterial adherence to oral biofilms to reduce adhesion, and therefore proliferation, of bacteria. Therefore it is used as a good option to deliver drugs such as antibiotics. Although not strictly having a toxic mechanism (9). Silica NPs possess a net positive charge on their surfaces, which promotes more interaction with the negatively charged surface of bacteria and shows efficient antimicrobial activity (23). The effect of silica nanoparticles and aqueous leaf extract on inhibition of the biofilm formation is may be due to that silica NPs subsequently may bind with DNA molecules and lead to disordering of the helical structure by cross-linking within and between the nucleic acid strands and also disrupt the biochemical processes and protein denaturation and cause cell death (48). Another proposed mechanism is, Colloidal SiO<sub>2</sub> NPs are usually negatively charged and hydrophilic (43). May be the SiO<sub>2</sub> NPs that may attach to the negatively charged bacterial cell wall and rupture it, thereby leading to protein denaturation and cause cell death. The different synthesis methods of SiO<sub>2</sub> NPs affect on the percentage (%) of biofilm inhibition for pathogenic bacteria, as shown in Table 5. SiO<sub>2</sub> NPs which synthesized by using cold plasma method achieved the highest biofilm inhibition percentage (62.68, 65%) for *S. aureus* and *E. coli* bacteria respectively.

**Table 5. The effect of different NPs and synthesis methods on biofilm inhibition percentage (%) for pathogenic bacteria**

Control	0.2773	0.2
Samples	Biofilm inhibition percentage (%)	
	<i>S. aureus</i>	<i>E. coli</i>
Aqueous leaf extract	56.73	37.5
Magnetic stirrer	47.23	28.33
Cold plasma	62.68	65

#### Antibacterial Activity

All the types of silica NPs did not showed any inhibition zone on the microorganisms by using well diffusion method and this behavior is in agreement with the results of Santra S. (45). Plants are abundant sources for natural and sustainable compounds, which are useful for green synthesis of nanostructures silica NPs. In this regard, we have been synthesis silica NPs via green method using *T. orientalis* aqueous leaf extract and by using TEOS as silica precursor. *T. orientalis* leaf extract contains bioactive compounds which can act as reducing and capping agent for biosynthesis of silica NPs. Prepared particles were surrounded with natural compounds from *T. orientalis* leaf extract. This matrix has hydrophilic functional groups that can make the particles colloiddally stable in aqueous environment without applying any harsh reaction condition. This synthesis condition is so interesting from the economical point of view for production of silica NPs in industrial scales.

#### ACKNOWLEDGMENT

The authors like to acknowledge the Central Environmental Laboratory, Physics Department, College of Science, University of Baghdad, and Physics Department, College of Women Science, University of Baghdad.

#### REFERENCES

1. Abass H. M. and M. F. Ahmad. 2012. *Staphylococcus aureus*. Diyala J. Agri. 6(2): 27-38
2. Adam F.; T. S. Chew and J. J. Andas. 2011. Sol-Gel. Sci. Technol. 59, 580-583
3. Alayande S.O.; E.O. Dare; W.B. Ayinde; J. Bamigbose; P. A Ayedun and G.A Osinkolu. 2012. Development of ordered and disordered macroporous silica from bagasse ash. African Journal of Pure and Applied Chemistry. 6, 10-14

4. Annu G. A. 2009. Rev. Mater. Res. 39, 49-69
5. Azlina H.N.; J.N. Hasnidawani; H. Norita and S.N. Surip. 2016. Synthesis of SiO<sub>2</sub> nanostructures using sol-gel method, ACTA Physica Polonica A. 129(4): 842-844
6. Boisen M. B.; G. V. Gibbs and M. S. T. Bukowinski. 1994. Framework silica structures generated using simulated annealing with a potential energy function based on an H<sub>6</sub>Si<sub>2</sub>O<sub>7</sub> molecule Sample: 17, Physics and Chemistry of Minerals 21, 269-284
7. Chatterjee S.; N. Zareena; S. Gautam; A. Soumyakanti; S. V. Prasad and S. Arun. 2007. Food Chem. 101, 515-523
8. Coradin T.; M. Boissière and J. Livage. 2006. Sol-gel Chemistry in Medicinal Science. In: Current Medicinal Chemistry. pp:13
9. Cousins B. G.; H. E. Allison; P. J. Doherty; C. Edwards; M. J. Garvey; D. S. Martin and R. L. Williams. 2007. Effects of a nanoparticulate silica substrate on cell attachment of *Candida albicans*. Journal of Applied Microbiology. 102, 757-765
10. Earle C. 1949. Platycladus orientalis. The Gymnosperm Database. pp:33
11. Ebrahiminezhad A.; S. Taghizadeh and Y. Ghasemi. 2017. Green synthesis of silver nps using mediterranean cypress (*cupressus sempervirens*) leaf extract, American Journal of Biochemistry and Biotechnology. 13(1): 1-6
12. Ebrahiminezhad A.; S. Rasoul-Amini; A. Kouhpayeh; S. Davaran; J. Barar and Y. Ghasemi. 2015a. Impacts of amine functionalized iron oxide nanoparticles on HepG<sub>2</sub> cell line. Curr Nanosci. 11: 113-119
13. Ebrahiminezhad A.; S. Rasoul-Amini; S. Davaran; J. Barar and Y. Ghasemi. 2014b. Impacts of iron oxide nanoparticles on the invasion power of *Listeria monocytogenes*. Curr Nanosci. 10: 382-388
14. Fayaz A. M.; K. Balaji; M. Girilal; R. Yadav; P. T. Kalaichelvan and R. Venketesan 2010. Nanomed. Nanotechnol. Biol. Med., 6, 103-109
15. Fridman A.; A. Chirokov and A. J. Gutsol. 2005. Phys D: Appl Phys 38(2): R1
16. Fridman G; Marie Peddinghaus; Manjula Balasubramanian; Halim Ayan; Alexander Fridman; xander Gutsol and Ari Brooks. 2006. Plasma Chem Plasma Process 26(4): 425-442
17. Fridman G.; A. Shereshevsky; M. Jost Monika; D. Brooks Ari; A. Fridman; A. Gutso; V. Vasilets and G. Friedman. 2007. Floating electrode dielectric barrier discharge plasma in air promoting apoptotic behavior in melanoma skin cancer cell lines: Plasma Chem Plasma Process. 27: 163–176
18. Ghorbani F.; Younesi H.; Mehraban Z.; Celik M.S.; Ghoreyshi A.A.; Anbia M. and J. Taiwan. 2013. Inst. Chem. Eng. 44, 821-828
19. Goh S. N.; A. Fernandez; S. Z. Ang; W. Y. Lau; D. L. Ng and E. S. G. Cheah. 2013. Effect of different amino acids on biofilm growth, swimming, motility and twitching motility in *Escherichia coli* BL<sub>21</sub>. Journal of Biology and Life Science. 4(2): 2157-6076
20. Grumezescu A. 2016. Nano Biomaterials in Antimicrobial Therapy: Applications of Nanobiomaterials. Chapter 9. Elsevier. 6, pp. 322
21. Gu S; J. Zhou; Z Luo; Q Wang and M Ni. 2013. Ind. Crops Prod. 50, 540-549
22. Hernández L. G.; D. A. Islas; P. A. R. Ortega; M. U. F. Guerrero and D. N. Enriquez. 2016. Journal of Nanomaterials & Molecular Nanotechnology. Green Synthesis, Characterization and Stabilization of Nanoparticles Silver with *Thuja Orientalis* Extract. 5(6):1-5
23. Jana R N.; M Earhart Christopher and Y. Ying Jackie. 2007. Synthesis of Water-Soluble and Functionalized Nanoparticles by Silica Coating. Chemistry of Materials. 19(21): 5074-5082
24. Jeon H. J.; S. C. Yi; and S. G. Oh. 2003. Preparation and antibacterial effects of Ag-SiO<sub>2</sub> thin films by sol-gel method. Biomaterials. 24, 4921–4928
25. Jilie K. and Y. U. Shaoning. 2007. Acta Biochim. Biophys. Sin. 39(8): 549-559
26. Joshi S. G.; M. Paff; G. Friedman; G. Fridman; A. Fridman and A. D. Brooks. 2010. Control of methicillin-resistant *Staphylococcus aureus* in planktonic form and biofilms: a biocidal efficacy study of nonthermal dielectric-barrier discharge plasma. Am. J. Infect. Control 38: 293–301
27. Karimipour M.; S. Mostoufirad; M. Molaei; H. R Nikabadi and A. G. Nesheli, 2016. Free reducing agent, one pot, and two steps synthesis of Ag@SiO<sub>2</sub> core-shells using

- microwave irradiatio. Journal of Nano-And Electronic. 8(3): 03020-1 - 03020-4
28. Khalid A. H. 2014. Structural and Optical Properties of Copper Nanoparticles Synthesized by Laser Ablation. Ph.D. Dissertation, Dept. of Physics, Coll. of Science, Univ. of Baghdad. pp.120.
29. Kogelschatz U. 2003. Plasma chem plasma Process 23(1):1-46
30. Kumar V.; D. K. Singh; S. Mohan and S. H. Hasan. 2016. Photo-induced biosynthesis of silver NPs using aqueous extract of *Erigeron bonariensis* and its catalytic activity against Acridine Orange. Journal of Photochemistry & Photobiology. B: Biology. 155, 39–50
31. Liou T. H. and C. C. Yang. 2011. Mater. Sci. Eng. B 176, 521-529
32. Lu M.M.D.; D. M. R. Silva; E. K. De Peralta and A.N. Fajardo. 2015. Philippine e-Journal for Applied Research and Development 5, 11-22
33. Macdonald I. D. G. and W. E. Smith. 1996. Langmuir, Orientation of cytochrome c adsorbed on a citrate-reduced silver colloid surface. 12, 706-713
34. Magesha H.; A. Kumara; A. Alama; Priyama, U. Sekarb; V. N. Sumantranc and R. Vaidyanathan. 2013. Identification of natural compounds which inhibit biofilm formation in clinical isolates of *Klebsiella pneumoniae*. Indian Journal of Experimental Biology. 51, 764-772
35. Mao Y.; W. Jiang; Sh. Wang; M. Liu; Sh. Xuan; X. Gong and K. Cham-Fai Leung. 2016. Mesoporous SiO<sub>2</sub> yolk shell confined core-satellite Ag nanoparticles: Preparation and catalytic activity. Journal of Alloys and Compounds. 680, 406-414
36. Mohd N. K.; N. N. A. N. Wee and A. A. Azmi. 2017. Green synthesis of silica nanoparticles using sugarcane bagasse. 3<sup>rd</sup> Electronic and Green Materials International Conference, 020123-1–020123-7
37. Montecinos S.; A. Cuniberti and A. Sepulveda. 2008. Materials Characterization. 59 (2):117–123
38. Mulvaney P. 1996. Surface plasmon spectroscopy of nanosized metal particles, Langmuir. 12, 788–800
39. Nath A.; A. Das; Sh. Deb; Ch. R. Bhattacharjee and J. Rout. 2015. Green Synthesis of Novel Antioxidant Luminescent Silica Nanoparticle Embedded Carbon Nanocomposites from a Blue-Green Alga. Green Processing and Synthesis. pp:1-13
40. Ojeda-Martínez M. L.; I. Yañez-Sánchez; A. Zamudio-Ojeda; F. J. Gálvez-Gastelum; R. Machuca-González and C. Velásquez Ordoñez 2013. SiO<sub>2</sub>-Ag<sup>0</sup> generation by sol-gel technique for antibacterial use, Digest Journal of Nanomaterials and Biostructures. 8(1): 409-414
41. Ow H.; D. R. Larson; M. Srivastava; B. A. Baird; W. W. Webb and U. Wiesner. 2005. Bright and stable core-shell fluorescent silica nanoparticles. Nano Lett. 5, 113-117
42. Pham D. Ph.; K. Kh. Huynh; C. V. Tran; V. Q. Vu and Th. Th. V. Tran. 2014. Preparation and structural characterization of sol-gel derived silver silica nanocomposite powders. International Journal of Materials Science and Applications. 3(5): 147-151
43. Pölloth C. F. 2012. The toxicological mode of action and the safety of synthetic amorphous silica-A nanostructured material. Toxicology. 294, 61-79
44. Prochnow A. M.; M. Clauson; J. Hong and A. B. Murphy. 2016. Gram positive and Gram negative bacteria differ in their sensitivity to cold plasma. Scientific Reports. 9(6): 21423-1 – 21423-11
45. Santra S. 2013. Ag Loaded Silica Nanoparticle/ Nanogel Formulation, Methods of Making, and Methods of Use, Patent Application Publication. pp:1-20
46. Seba H. Y. and R. Cherfi. 2015. Effect of hydrogen on boron doped amorphous silicon prepared by dc magnetron sputtering. 18, 229-239
47. Sharma G.; A. R. Sharma; M. Kurian; R. Bhavesh; J.S. Nam and S. S. Lee. 2014. Green synthesis of silver nanoparticle using *myristica fragrans* (nutmeg) seed extract and its biological activity, Digest Journal of Nanomaterials and Biostructures. 9(1): 325-332
48. Sravanthi M.; D. M. Kumar; B. Usha; M. Ravichandra; M. M. Rao and K. P. Hemalatha. (2016). Biological synthesis and characterization of copper oxide nanoparticles using antigonon leptopus leaf extract and their antibacterial activity. Biotechnol. Tech. 4(8): 589-602

49. Srivastava P.; P. Kumar; D.K. Singh and V.K. Singh. 2012. Biological properties of *Thuja orientalis* Linn. *Advances in Life Sciences* 2: 17-20
50. Tan W. H.; K. M. Wang; X. He; X. J. Zhao; T. Drake; L. Wang and R. P. Bagwe. 2004. Bio nanotechnology based on silica NPs. *Med. Res. Rev.* 24, 621- 638
51. Varshney VK and S. Naithani. 2011. Cellulose Fibers: Bio- and Nano-Polymer Composites. 43-61
52. Wang D. and G. P. Bierwagen. 2009. Sol-gel coatings on metals for corrosion protection. In: *Progress in Organic Coatings* 64, 327-338
53. Zhang N.; D.K. Park and H.J. Park. 2013. Hair growth-promoting activity of hot water extract of *Thuja orientalis*. *BMC Complementary and Alternative Medicine.* 13: 1-11
54. Zhang S. and N. Ali. 2007. *Nanocomposite Thin Films and Coatings: Processing, Properties and Performance.* Imperial College press. 1-628